LABORATORY

TECHNIQUE

SETUP FOR STUDYING VORTEX FLOW ON THE SURFACE OF A LAYER OF LIQUID 4HE IN NORMAL AND SUPERFLUID STATES

© 2025 A. A. Levchenko, L. P. Mezhov-Deglin, I. A. Remizov,

P. G. Selin*, M. R. Sultanova

Yu.A. Osipyan Institute of Solid State Physics of the Russian Academy of Sciences

Russia, Chernogolovka, Moscow region

**e−mail: selin@issp.ac.ru*

Received June 26, 2024

Revised July 26, 2024

Accepted October 15, 2024

Abstract. The design of the setup intended for studying the interaction features of vortex flows generated by capillary-gravity waves on the surface of liquid helium 4He in normal and superfluid states with injected charges is described. An example of the results of studying the influence of vortex flows generated by waves in a layer of superfluid helium He-II 2.5 cm deep at temperatures T ≥ 1.5 K on the distribution of negative ion currents over five segments of a receiving collector immersed in the liquid is given.

DOI: 10.31857/S00328162250117e2

1. INTRODUCTION

It is known (see, for example, [1-8]) that a free electron injected into liquid ^{4}He localizes in the liquid volume in a vacuum cavity - an electron bubble with a radius of about 17 Å at saturated vapor pressure. These negatively charged nanoparticles (negative ions) can be attempted to be used as tracer particles in studying not only classical but also quantum turbulence generated by nonlinear capillary waves on the surface of superfluid He-II (quantum Bose liquid [3, 7, 9, 10-13]).

As shown previously (see, for example, [3, 4]), when quantum vortices are excited in superfluid He-II cooled below a temperature of 1.0 K, negative ions become localized near the vortex core. The binding energy of the electron bubble with the vortex filament (the depth of the potential well U_q) is $U_q \approx 50$ K, and in weak electric fields with strength $E \leq 30$ V/cm, one can observe the movement of charged tangles of quantum vortices in the liquid. As the temperature of He-II increases to 1.65 K, the

binding energy of negative ions with quantum vortices first gradually decreases several times, and then drops sharply in a narrow temperature range of 1.65 - 1.70 K, so that at temperatures above 1.7 K, the binding energy $U_q \leq 2$ K and negative ions, which move in the bulk of He-II under the influence of an applied electric field, are practically not captured by quantum vortices.

In [14], it was shown that nonlinear interaction between non-collinear capillary waves propagating on the surface of a liquid layer leads to the generation of vortex flow beneath the layer's surface. We used the methodology described in this article to excite vortex flows on the surface of a helium layer in both normal He-I and superfluid He-II states [15-18].

The second section describes the design of the setup intended for studying the features of interaction between vortex flows generated by capillary-gravitational waves on the surface of liquid ^{4}He with injected charges. The measurement methodology is also presented there. The third section shows one of the results of test trials of the setup's functionality. The conclusion briefly summarizes the results of the work done.

2. SETUP DESIGN AND MEASUREMENT METHODOLOGY

The layout of the main units of the setup within the vacuum cavity of the optical cryostat is shown in Fig. 1a. Next to it is a photograph of the metal helium cryostat [16], equipped with flat optical windows made of quartz glass *7* (Fig. 1b). A vertically oriented cylindrical container *1* , which houses the working cell, is mounted on four copper cold conductors *6* (Fig. 1a) in the vacuum cavity of the cryostat. The container *1* is surrounded by a cold copper shield *5* , attached to a copper ring at the bottom of the cryostat's helium bath. The helium shield is surrounded by a nitrogen shield *4* , which is mounted on the walls of the cryostat's nitrogen bath. Flat quartz windows installed on the nitrogen and helium shields, and external vacuum-tight windows *7* , which were attached to cylindrical extension tubes welded to the cryostat shell (*7* in Fig. 1b), allow monitoring the movement of the liquid helium level in the working cell.

The method of recording waves excited by oscillating flat wave generators on the surface of the helium layer in the working cell is described in detail in [17]. A laser beam from an external light source *9* in Fig. 1 **a** directed at the surface of the liquid layer was reflected from the free surface of the layer and reached the optical sensor *10* in Fig. 1 **a** , the output of which was connected to an external computerized system for recording and processing measurement results. By the amplitude of oscillations of the reflected beam, it was possible to determine the amplitude of the waves excited on the liquid surface.

Fig. 1. **a** – Schematic of the cryogenic part of the facility... **b –** photograph of the cryostat

The design of the working cell, which is placed inside a vertically oriented cylindrical container, is shown in Fig. 2 **c** . The container *1* made of stainless steel with an internal diameter of 150 mm and a height of 100 mm (wall thickness 3 mm) is equipped with a transparent upper window *2* with a thickness of 3 mm, made of fused quartz. For vacuum-tight connection of the quartz window *2* to the upper flange of the container, as well as the copper clamping disk *3* to the lower flange, as well as windows *7* in Fig. 2a, malleable indium rings were used. The container is surrounded by a cold shield (Fig. 1a) and connected to the bottom of the cryostat's helium bath using four copper rods, which simultaneously served as thermal conductors. Gaseous ^{4}He was condensed into the container from an external transport Dewar vessel through a filling capillary (the entry point of the capillary into the container is indicated in Fig. 2c), which first passed through the cryostat's helium bath and was equipped with a fine-porous copper filter to prevent foreign solid suspensions from entering the cell volume. The liquid was filled until its surface reached the edge of the lateral faces of the cell (the liquid level was registered with an accuracy of about 0.1 mm). The temperature of liquid helium in the cryostat bath and, consequently, in the container and working cell was lowered to 1.5 K by pumping liquid helium vapor from the bath with an external pump. Changes in the temperature of liquid helium in the working cell were monitored using a semiconductor thermometer installed on the outer wall of the container, as shown in Fig. 2c.

Fig. 2. **a –** Sketch of the container with the experimental cell; **b –** diagram of the experimental cell; **c** – photograph of the cell inside the container

The working cell shown schematically in Fig. 2a, b was fixed inside the container on eight vertical brass studs with a height of 70 mm and a diameter of 3 mm. The studs were pre-screwed into a specially machined annular belt in the lower part of the container. As can be seen in Fig. 2b, the working cell was a rectangular parallelepiped with internal dimensions of 50×50×30 mm ^{3} . The flat side faces and bottom of the cell fixed on the studs were made of 2 mm thick duralumin sheet. All metal faces were electrically insulated from the studs and from each other by quartz washers. The upper face of the cell *4* (Fig. 2a) was made of quartz glass. A semi-transparent metal film was pre-deposited on the lower surface of the quartz face. During measurements, the distance from the liquid helium surface in the cell to the lower surface of the quartz face was 3 mm. The radioactive source of injected charges in helium *11* (titanium tritide film on a metal substrate) was installed on one of the vertical side faces of the cell (Fig. 2a). The source diameter is 3 mm, the average energy of β-particles emitted by the source is close to 5 keV, the maximum is approximately 18 keV. Under irradiation, a plasma of free electrons and positively charged helium ions was formed in a liquid layer with a depth

of about 10 μm near the charge source. By applying negative voltages to the face where the source was installed, negative charges could be injected into the bulk of liquid helium.

In the series of first experiments [15], the charge source was installed on the face opposite to the receiving collector. When upgrading the setup, we moved the source to an adjacent face [18]. Changing the location of the source made it possible to obtain a more uniform field configuration and increase the field strength near the charge source, which, in turn, allowed increasing the flow of charges coming to the collector. Collector *10* (Fig. 2a, b) was made from a sheet of copper-clad fiberglass laminate. The outer side of the collector was glued to the duralumin face with BF-4 adhesive and electrically isolated from the metal face. Four tracks 1 mm wide were pre-etched on the copper coating. Thus, the receiving collector consisted of five electrically isolated vertically oriented receiving segments with linear dimensions of 9×30 mm ^{2}, on the surface of which a gold film was additionally deposited before assembling the cell.

Each collector segment was connected to an independent current amplifier (Fig. 3). The design of the current amplifiers is described in [19]. During the experiments, the total collector current at various field configurations did not exceed 5000 fA. All electrical wires connecting the parts located inside the container *1* (Fig. 1a) with external current amplifiers and voltage sources of the control and data acquisition system passed through hermetic connectors with glass insulation, which were located at the bottom of the container *3* (Fig. 2a).

Fig. 3. Electrical block-diagram of the setup

To excite mutually perpendicular waves on the free surface of the liquid in the cell, two flat metal plungers [14, 15, 18] were used (wave generators *8* in Fig. 2), the bases of which were fixed to the lower part of two adjacent side faces. The characteristic dimensions of the plungers were 1×3×40 mm ^{3}. The plungers were positioned at a distance of 3 mm from the surface of the face. Each plunger was driven by its own electromagnetic drive, with alternating sinusoidal voltage supplied from a two-channel function generator (see the diagram in Fig. 3). The phase difference between the alternating voltages fed to the plungers was 90º. The coil controlling the plunger movement was installed in a special recess (pocket) on the side wall of the container *7* (Fig. 2c), and a neodymium magnet cube *9* (Fig. 2a) was attached to the plunger leg opposite the coil with BF-4 glue. The plungers performed reciprocating movement in the horizontal plane along the surface of the liquid helium layer. The drive pumping frequency f_g in different experiments was f_g = 20–50 Hz. As in [17], the amplitude and steepness of the waves generated on the liquid surface were estimated from the measurements of the oscillation amplitude of a laser beam reflected from the liquid surface in the cell (the laser and

receiving detector were located outside, opposite the cryostat windows, as shown in Fig. 1). According to our estimates, in most of the measurements conducted with pumping at a frequency of $f_g = 49.9$ Hz, the amplitude of the standing capillary waves reached $H \approx 0.02$ mm, the wave steepness reached $kH \approx 0.06$, where k is the wave vector.

As shown in Fig. 3, the collector currents recorded by each of the five collector segments pass through independent current amplifiers, then enter an analog-to-digital converter (ADC), and then the digitized signal enters the computer memory via the PCI (peripheral component interconnect) bus.

A constant electric voltage, which was applied to different faces of the parallelepiped (Fig. 2b), came from five independent DC voltage sources with a common ground [20]. The voltage values on each cell face could be changed from zero to –450 V, thereby creating various configurations of the applied electric field, in which negative ions moved in the volume of liquid helium from the charge source to the receiving collector.

By adjusting the voltage distribution on the lower U_{down} and upper U_{up} faces of the cell, it was possible to set the magnitude and direction of the perpendicular component of the applied electric field $E_{\perp} \sim \Delta U_{\perp}/L = |U_{\text{down}} - U_{\text{up}}|/L$, where $L = 3$ cm − the depth of the liquid layer in the cell. This made it possible to "press" the injected charges moving in the liquid from the source to the collector either to the free surface of the liquid or to the bottom of the cell, in order to enhance (or minimize) the influence of vortex flows generated by waves on the layer surface on the distribution of currents across various segments of the receiving collector. The output signals from the current amplifiers $I_i(t)$ ($i = -2, -1, 0, +1, +2$) were digitized using an ADC and recorded in the computer memory (Fig. 3). To isolate the constant component of the current $I_i(t)$ against the background of interference from alternating fields arising when the plunger oscillations were turned on, the recorded dependencies $I_i(t)$ were subjected to Fourier filtering at low frequencies.

3. RESULTS OF TEST TRIALS

Figure 4 shows an example of the test results for the installation's performance, which illustrates how the distribution of negative ion currents across the five segments of the receiving collector $I_i(T)$ and the total collector current $I_{\text{sum}}(T)$ change with increasing liquid temperature from 1.5 to 2.19 K when the wave pumping is turned off (dashed curves) and turned on (solid curves) at a frequency of $f_g = 49.9$ Hz. The length of the capillary wave excited on the liquid layer surface is $\lambda \approx 0.2$ cm, and the steepness of the capillary waves is $kH \approx 0.05$.

Fig. 4. Solid curves describe the temperature dependence of negative ion currents registered by the central segments when the wave pumping is on; dashed curves - in the absence of pumping

The magnitude and distribution of constant voltages applied to the faces of the working cell are the same with the pumping turned off and on: the voltage at the source $U_{source} = U_{s2} = -100$ V, on the lateral face opposite to the source, the voltage is $U_{s1} = 0$, the voltage on the upper face is $U_{up} = -50$ V, and on the lower face $U_{down} = -100$ V. The collector is at zero potential. Negative ions moving from the charge source to the collector are pressed by the vertical component of the applied electric field to the free surface of the liquid layer $E_{\perp} \sim | U_{down} - U_{up} | / L \sim 17$ V/cm .

It can be seen that with a smooth increase in temperature of the pre-cooled He-II layer from 1.5K to 2.19K, the distribution of negative ion currents across the segments of the receiving collector with wave pumping turned on changes significantly in a narrow temperature range near 1.7K, in contrast to the current distribution across segments in the absence of pumping. This may be due to the fact that at temperatures near 1.7K, the probability of capturing electron bubbles moving in a weak longitudinal electric field by quantum vortices generated by non-collinear capillary waves decreases exponentially compared to the probability of capturing electron bubbles by quantum vortices at He-II temperatures below 1.7K [8], i.e., negative ions injected into superfluid helium can serve as tracer particles for detecting quantum vortices in He-II.

At temperatures above 1.7K, where the capture of negative ions by quantum vortices can be neglected, the main role should be played by elastic scattering of injected charges on vortex structures, such as vorticity ridges, which form in the volume of the normal component of He-II, just as in the volume of He-I at $T > T_{\lambda}$, as a result of interaction between ordinary, classical vortices generated by nonlinear waves on the surface of the liquid layer [10, 11], as well as scattering on tangles of quantum vortices arising in the volume of the superfluid component of He-II as a result of strong interaction (friction) between the normal and superfluid components at temperatures above 1K.

4. CONCLUSION

The installation, the design of which is described in this article, allows for the excitation of capillary-gravity waves on the surface of a liquid ^{4}He and study of the interaction of negative charges (electron bubbles) injected into liquid helium with vortices generated by these waves, in a wide temperature range from 4 to 1.5 K. Significant changes in the distribution of negative ion currents across the central segments of the receiving collector with a smooth increase in the

temperature of the liquid layer in a narrow range near 1.7 K with wave pumping on (Fig. 4) may be associated with a change in the mechanism of interaction between electron bubbles and quantum vortices. This allows us to assert that nonlinear capillary waves propagating on the surface of a superfluid excite not only classical but also quantum vortices, i.e., the installation developed and manufactured by us is suitable for studying both classical and quantum turbulence in superfluid He-II.

ACKNOWLEDGMENTS

The authors are grateful to A.V. Lokhov for assistance in creating and testing the installation.

FUNDING

The work was carried out within the framework of the state assignment of the Institute of Solid State Physics of the Russian Academy of Sciences.

REFERENCES

1. *Shikin V.B.* // Sov. Phys. Usp. 1977. V. 121. P. 457.
2. *Shikin V.B., Monarkha Yu.P.* Two-dimensional charged systems in helium. Moscow: Nauka, 1989.
3. *Glaberson W.I., Strayer D.M., Donnelly R.J.* // Phys. Rev. Lett. 1968. V. 20. P. 1428. https://doi.org /10.1103/PhysRevLett.20.1428
4. *Pratt W.P., Zimmermann W., Jr.* // Phys. Rev. 1969. V. 177. P. 412. https://doi.org/10.1103/PhysRev.177.412
5. *Keshishev K.O., Kovdrya Yu.Z., Mezhov-Deglin L.P., Shalnikov A.I.* // JETP. 1969. V. 56. P. 94.
6. *Aitken F., Bonifaci N., von Haeften K., Eloranta J.* // J. Chem. Phys. 2016. V. 145. P. 044105. http://dx.doi.org/10.1063/1.4959293
7. *Aitken F., Bonifaci N., Mendoza-Luna L.G., von Haeftenb K.* // Phys. Chem. Chem. Phys. 2015. V. 17. P. 18535. https://doi.org/10.1039/C5CP02539G
8. *Walmsley P.M., Levchenko A.A., Golov A.I.* // Journal of Low Temperature Physics. 2006. V. 145. P. 143. https://doi.org/10.1007/s10909-006-9235-3
9. *Andreev A.F., Kompaneec D.A.* // JETP. 1971. V. 61. P. 2459.
10. *Borghesani A.F.* // International Series of Monographs on Physics. 2007. V. 137. P. 560.
11. *Walmsley P.M., Golov A.I., Hall H.E., Levchenko A.A., Vinen W.F.* // Phys. Rev. Lett. 2007. V. 99. P. 265302. https://doi.org/10.1103/PhysRevLett.99.265302

12. *Eltsov V.B., de Graaf R., Hänninen R., Krusius M., Solntsev R.E., L'vov V.S., Golov A.I., Walmsley P.M.* // Progress in Low Temperature Physics: Quantum Turbulence. V. 16. P. 46. https://doi.org/10.1016/S0079-6417(08)00002-4
13. *Landau L.D., Lifshitz E.M.* Theoretical Physics. Vol. VI. Hydrodynamics, Moscow: Nauka, 1986.
14. *Filatov S.V., Parfenyev V.M., Vergeles S. S., Brazhnikov M.Yu., Levchenko A.A., Lebedev V.V.* // Phys. Rev. Lett. 2016. V. 116. P. 054501. https://doi.org/10.1103/PhysRevLett.116.054501
15. *Remizov I.A., Sultanova M.R., Levchenko A.A., Mezhov-Deglin L.P.* // Low Temp. Phys. 2021, V. 47. P. 378. https://doi.org/10.1063/10.0004229
16. *Dite A.F., Mezhov-Deglin L.P., Revenko V.I.* // PTE. 1979. № 6. P. 160.
17. *Brazhnikov M.Yu., Levchenko A.A., Mezhov-Deglin L.P.* // IET. 2002. V. 45. № 6. P. 31. https://doi.org/10.1023/A%3A1021418819539
18. *Sultanova M.R., Remizov I.A., Mezhov-Deglin L.P., Levchenko A.A.* // JETP Letters. 2023. V. 118. P. 596. https://doi.org/10.31857/S1234567823200089
19. *Remizov I.A., Mezhov-Deglin L.P., Sultanova M.R.* RF Patent 2754201, 2021.
20. *Remizov I.A., Mezhov-Deglin L.P., Sultanova M.R.* RF Patent 2783476, 2021.

FIGURE CAPTIONS

Fig. 1. **a** - Scheme of the cryogenic part of the installation: *1*- cylindrical container, *2* - helium bath of the cryostat, *3* - nitrogen bath, *4* - nitrogen shield, *5* - helium shield, *6* - copper cold conductors, *7* - quartz optical windows, *8* - bottom of the helium bath of the cryostat, *9* - helium laser, *10* - semiconductor bolometer, **b** - photograph of the cryostat.

Fig. 2. **a -** Sketch of the container with the experimental cell; **b -** scheme of the experimental cell; **c** - photograph of the cell in the container volume: *1* - cylindrical container, *2* - clamping transparent window made of quartz glass, *3* - copper disk, *4* - transparent upper face of the working cell, *5* and *6* - lower face and vertical side faces of the cell, *7* - electromagnetic coil, *8* - plungers, *9* - neodymium magnet, *10* - receiving five-segment collector, *11* - charge source, *12* - copper bushings for fastening cold conductors, *13* - washer for fastening the resistive thermometer, *14* - inlet of the capillary of the system for filling the container with cold ^{4}He.

Fig. 3. Electrical block diagram of the installation.

Fig. 4. Solid curves describe the temperature dependence of negative ion currents registered by the central segments -1 (green curve) and 0 (purple curve) of the receiving collector with wave pumping turned on at a frequency of $f_g = 49.88$ Hz. The currents registered by segments -2, 1 and 2, are small and weakly dependent on temperature. The blue curve describes the temperature dependence of the total current of the receiving collector I_{sum}.

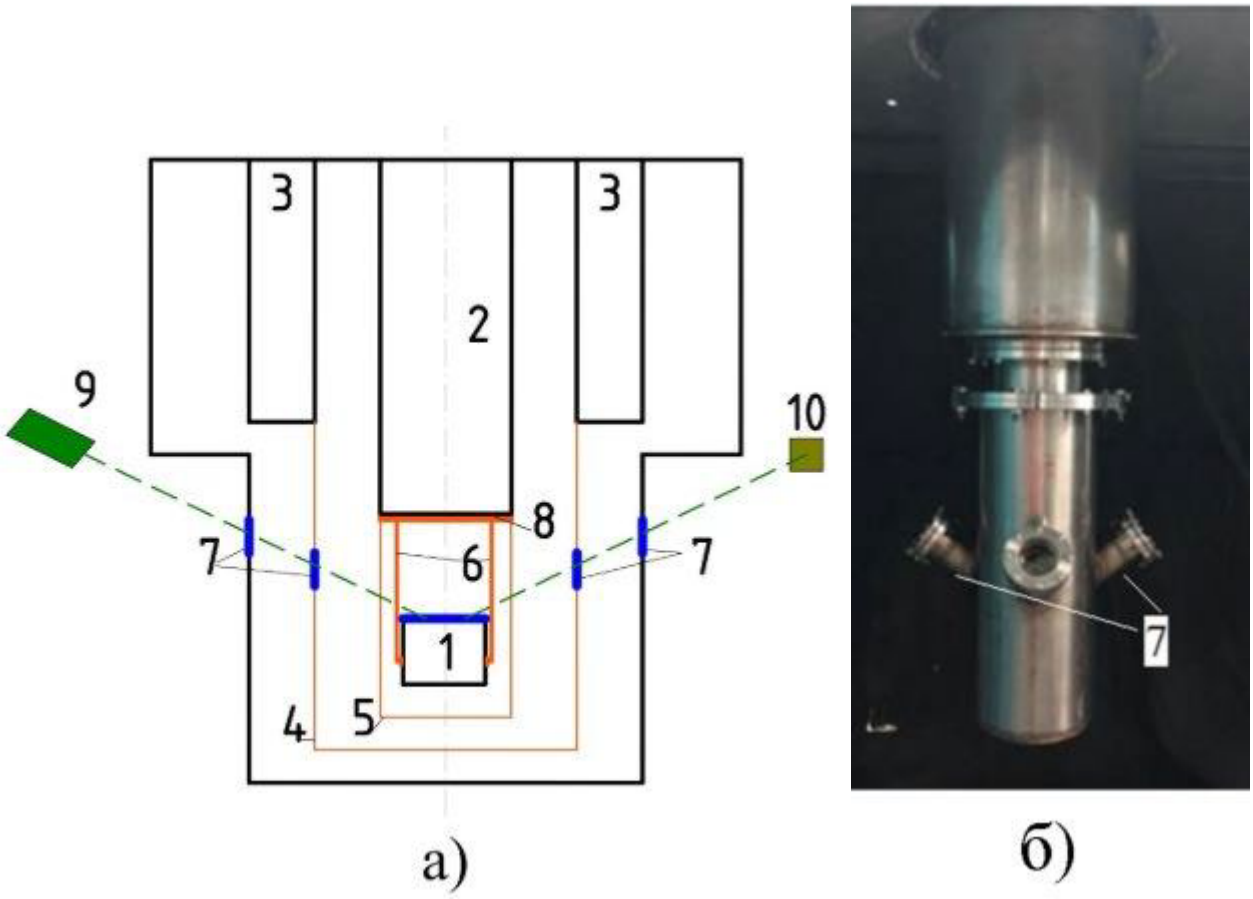

Fig. 1.

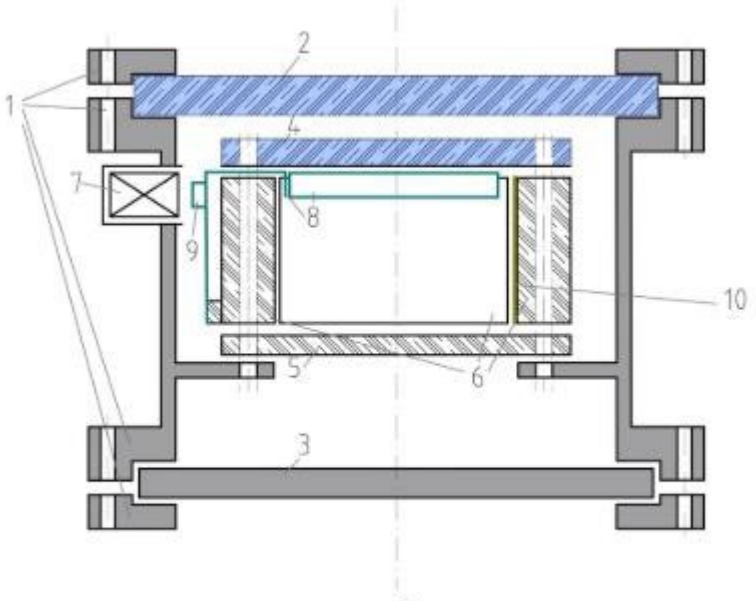

а)

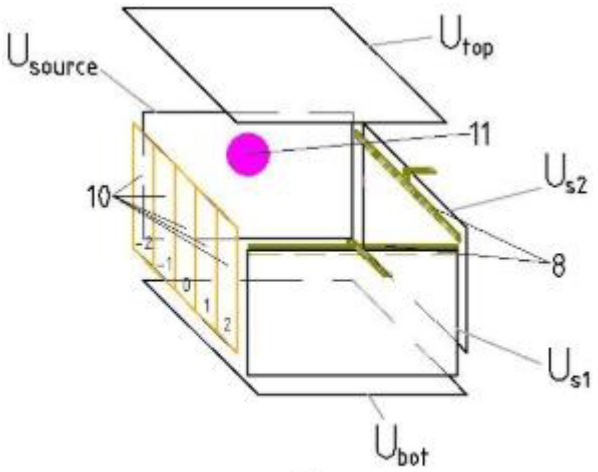

б)

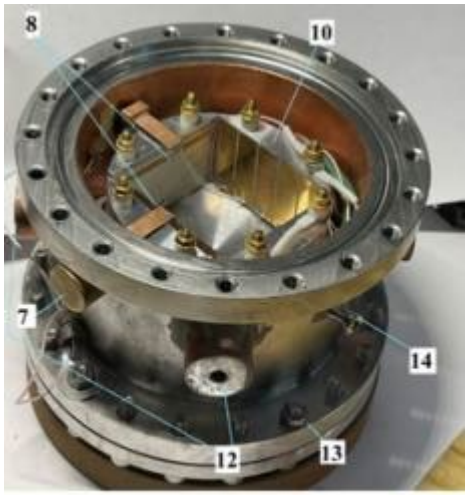

в)

Fig. 2.

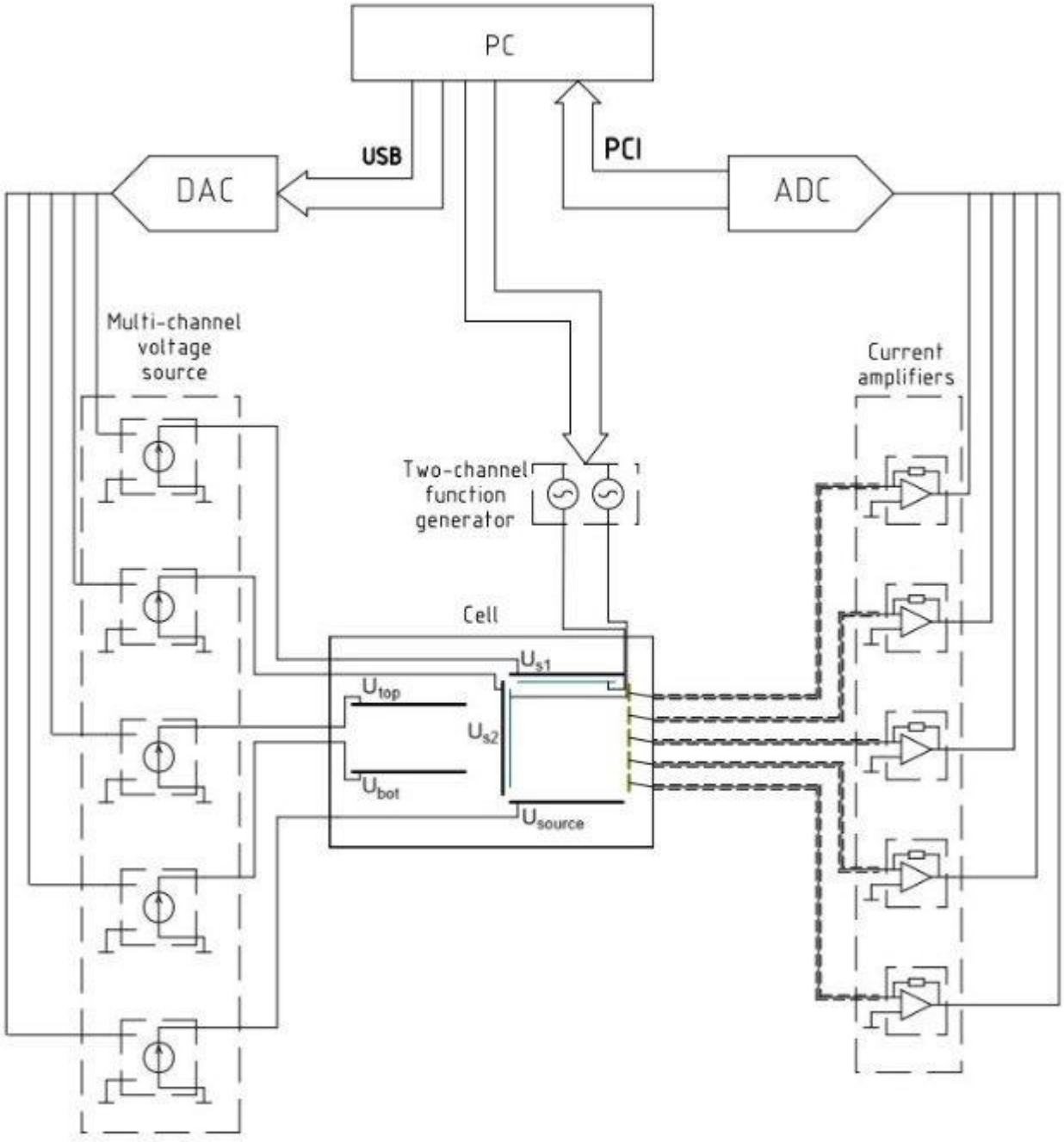
PC
USB
PCI
DAC
ADC
Multi-channel
voltage
source
Current
amplifiers
Two-channel
function
generator
Cell
U_{s1}
U_{top}
U_{s2}
U_{bot}
U_{source}

Fig. 3.

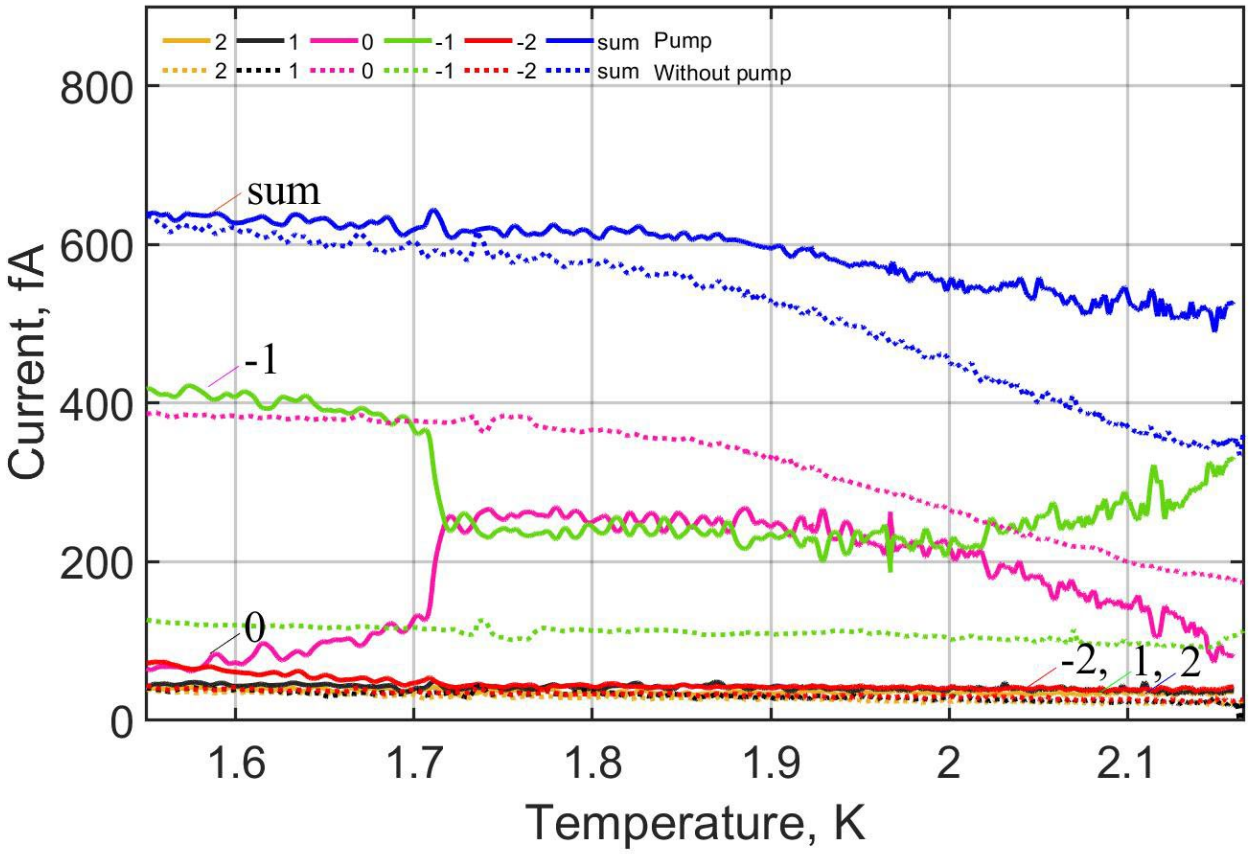
2
1
0
-1
-2
sum Pump
2
1
0
-1
-2
sum Without pump
800
600
400
200
0
Current, fA
sum
-1
0
-2, 1, 2
1.6
1.7
1.8
1.9
2
2.1
Temperature, K

Fig. 4.